

INVESTIGATIONS ON THE SPATIAL ARC RESISTANCE DISTRIBUTION OF AN AXIALLY BLOWN SWITCHING ARC

M. WEUFFEL^{1*}, P. G. NIKOLIC¹ AND A. SCHNETTLER¹

¹ Institute for High Voltage Technology, RWTH Aachen University, 52056, Aachen, Germany
*weuffel@ifht.rwth-aachen.de

ABSTRACT

The determination of the spatial arc resistance distribution is one option to gain deeper insight into the physical processes during current interruption in high voltage circuit breakers. A measurement system capable of measuring this spatial arc resistance distribution by means of capacitive field probes is applied to a circuit breaker model equipped with a Laval nozzle geometry which has previously been investigated using optical measuring methods. According to these investigations, which serve as reference case, the spatial arc resistance distribution is determined for varying current steepness values. Comparing the results a general agreement between the determined arc resistance distributions and the results from the reference case is observed. The functionality of the measurement system is confirmed for both successful and non-successful switching operations. Uncertainties and differences in the obtained arc resistance distributions are discussed.

1. INTRODUCTION

The ongoing optimization of today's switching technologies requires a deep understanding of the physical processes during the interruption process in high voltage circuit breakers. One of the aspects related to the interruption capability of gas blast circuit breakers is the spatial arc resistance distribution of the switching arc which can provide insight into the cooling processes during current interruption. A measurement system, which allows the contactless and non-invasive determination of the spatial arc resistance distribution of an axially blown switching arc by means of capacitive field probes, is applied to a Laval nozzle geometry

and analyzed concerning the quality and accuracy of the results [1]. For this purpose the nozzle geometry is chosen from a reference case providing detailed information on the arc resistance characteristics from investigations using other optical measurement techniques [2]. The arc resistance distribution is determined in experimental investigations with different values for the current steepness di/dt .

2. MEASURING PRINCIPLE

The measuring principle for the indirect measurement of the spatial arc resistance distribution is based on the electrical field surrounding the arc and is schematically depicted in figure 1. The investigated arc burns between two arcing electrodes inside an insulation nozzle. The axial arc resistance distribution is assumed to be describable by a series connection of n single resistors R_i where each value R_i corresponds to a voltage drop along the axis of the arc.

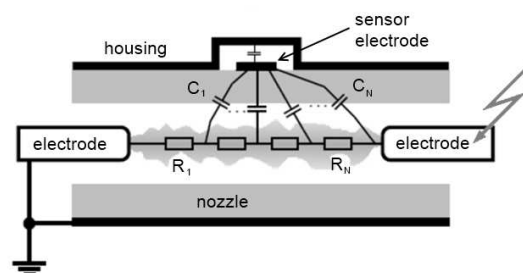


Fig. 1 Measuring principle (sketch) [3]

By measuring the potential drop along the arc axis the resistance distribution can be determined taking the total current into account. In order to measure the arc potential, a sensor electrode is placed between the cylinder and the nozzle. A conductive shielding housing which is mounted around the nozzle is connected to ground and serves as reference potential. Between the sensor electrode and the grounded housing a capacity C_e

occurs. This results in a capacitive field probe. Placing multiple sensors along the axis of the arc allows the determination of the potential distribution. Each sensor measures a partial voltage of the arc [3].

3. EXPERIMENTAL SETUP

A test device with a Laval nozzle geometry according to the reference case is used for the arc resistance measurements (see figure 2). As quenching gas nitrogen (N_2) at a constant blowing pressure of 10 bar (abs.) is used.

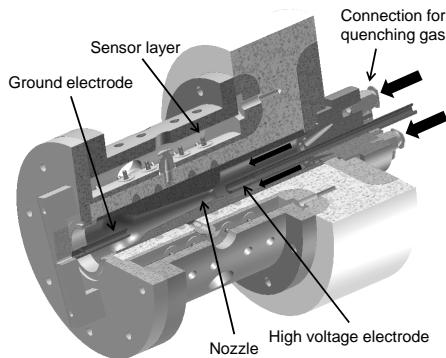


Fig. 2 Cross-sectional view of the circuit breaker model

The investigated nozzle is made of polytetrafluorethylen (PTFE). Arc ignition is achieved by means of an ignition wire. In order to avoid a virtual enlargement of the high voltage electrode, i.e. accumulation of hot gas surrounding the high voltage electrode, both the ground and the high voltage electrode are drilled out so that hot gas in front of the arcing electrodes can pass through [1]. The field probes for the determination of the arc resistance distribution are arranged in multiple layers along the arc axis with groups of four probes per layer.

According to the reference case the test current is generated with a pulse forming network providing a rectangular shaped current of several milliseconds duration with a variable current steepness towards current zero (see figure 3) [2].

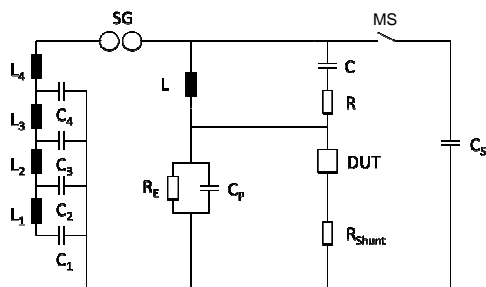


Fig. 3 Test circuit according to the reference case [2] (DUT: Device under test, SG: Ignition spark gap, MS: Making switch)

Inductances $L_1 \dots L_4 = 1.9$ mH and capacitors $C_1 \dots C_4 = 0.7$ mF are selected. The remaining elements are $C_P = 17.3$ nF, $R_E = 19.5$ M Ω , $C_S = 0.71$ mF, $C = 97.7$ nF and $R = 0.87$ k Ω . Two inductances with $L = 0.22$ mH and $L = 0.525$ mH are available in order to adjust the prospective steepness di/dt of the test current towards current zero crossing. Thus both successful and non-successful current interruption experiments are achieved and investigated. The resulting shape of the test current and arcing voltage is shown exemplarily in figure 4. In this example the circuit breaker model is not able to interrupt the test current in the first current zero crossing (i.e. a thermal re-ignition), but only in the second current zero crossing at $t \approx 1$ ms.

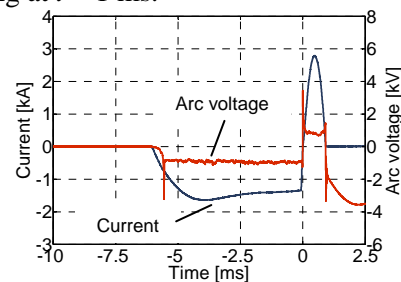


Fig. 4 Exemplary test current and arc voltage

4. DETERMINATION OF THE SPATIAL ARC RESISTANCE DISTRIBUTION

For the evaluation of the arc resistance measurements according to the reference case the contact gap is divided into five different arc sections. These arc sections, their particular length and the corresponding axial positions of the sensor layers are depicted in figure 5. Section *a* corresponds to the laminar flow section upstream of the nozzle throat, sections *b* – *e* correspond to the turbulent flow section downstream of the nozzle throat [2].

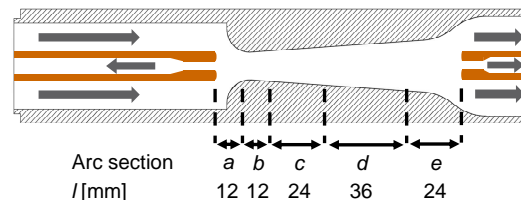


Fig. 5 Cross-sectional view of the investigated nozzle with arcing electrodes, direction of gas flow and defined arc sections *a* – *e*

The waveform of a measured arc current, arc voltage and the total arc resistance is depicted in figure 6 for a successful current interruption with use of the inductance $L = 0.525$ mH and a resulting current steepness of $di/dt = 6.46$ A/ μ s.

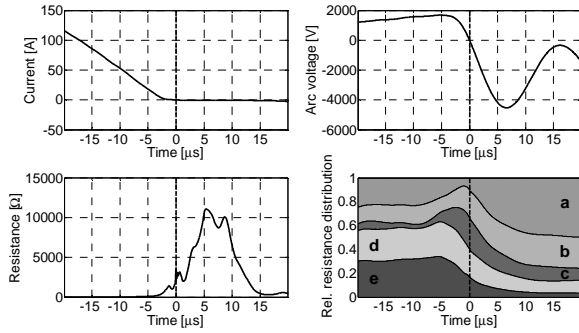


Fig. 6 Measured current, arc voltage and total arc resistance with determined relative axial resistance distribution for successful current interruption ($di/dt = 6.46 \text{ A}/\mu\text{s}$)

The determined relative axial arc resistance distribution is additionally shown by means of the band diagram in which the relative resistance of each arc section is represented by the width of the corresponding band. Since the sum of all arc section resistances is equal to the total arc resistance, the sum of all bands is always equal to 1. From the relative resistance distribution it is observed that during the high current phase until $t \approx -8 \mu\text{s}$, the laminar arc resistance (section *a*) is about 20 – 25 % of the total arc resistance. From $t \approx -8 \mu\text{s}$ the relative resistance in the laminar arc section decreases and the resistance in the turbulent arc sections (especially sections *b* and *c*) increases significantly. The resistance of the arc section in front of the ground electrode (section *e*) is decreasing from more than 30 % during the high current phase to less than 5 % after current zero. After current interruption ($t > 0 \text{ s}$) the laminar arc resistance (section *a*) increases to almost 50 % of the total resistance.

In comparison to this, the waveform of an arc resistance measurement for a non-successful current interruption due to a thermal failure is depicted in figure 7. Due to the use of the inductance $L = 0.22 \text{ mH}$ a significantly higher current steepness $di/dt = 22.6 \text{ A}/\mu\text{s}$ is achieved. From the relative axial arc resistance distribution it is observed that during the high current phase until $t \approx -5 \mu\text{s}$, the laminar arc resistance in section *a* is about 40 % of the total arc resistance, whereas the turbulent sections *b* and *c* are about 20 % of the total resistance. Towards current zero, the relative laminar arc resistance decreases to less than 10 % at $t \approx 2 \mu\text{s}$ and sections *b* and *c* account for the dominating percentage of the arc resistance with about 40 % of the total arc resistance. After the thermal re-ignition at $t \approx 2 \mu\text{s}$ the relative resistance of sections *a* and *b* increases significantly while the resistance of the other arc sections *c*, *d* and *e* decreases. Especially

the relative resistance of the turbulent arc section *c* decreases to less than 5 % of the total arc resistance. In contrast to this, the laminar arc resistance in section *a* increases to almost 60 % of the total arc resistance.

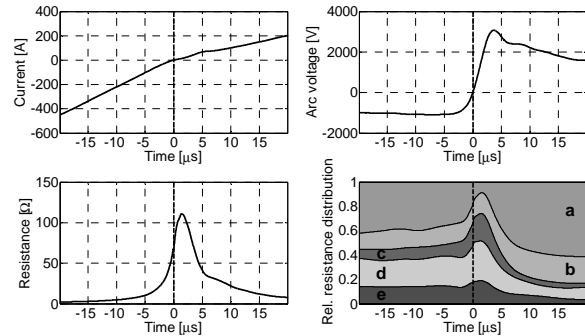


Fig. 7 Measured current, arc voltage and total arc resistance with determined relative axial resistance distribution for non-successful current interruption due to thermal failure ($di/dt = 22.6 \text{ A}/\mu\text{s}$)

5. ANALYSIS AND COMPARISON TO THE REFERENCE CASE

During the previous investigations in the reference case, experimental test series with di/dt values in the range of $di/dt = 20 \dots 50 \text{ A}/\mu\text{s}$ at a quenching gas pressure of 23 bar are performed with an investigated nozzle geometry similar to the nozzle used for the experiments presented in the context of this contribution. A comparison of the laminar arc section resistance characteristics in relation to the total arc resistance is depicted in figure 8. From both the experimental results and the results from the reference case it is observed that during the high current phase the dominating percentage of the arc resistance is obtained in the laminar arc section *a*. First in the vicinity of current zero, the contribution of the laminar arc section to the total arc resistance decreases. In contradiction to the results from the reference case, it is indicated in the present investigations that at $t > 2 \mu\text{s}$ after current interruption the contribution of the laminar arc section to the total resistance increases again.

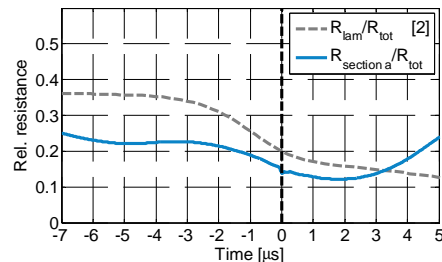


Fig. 8 Relative arc resistance in laminar arc section for successful current interruption from [2] and from test series with $L = 0.22 \text{ mH}$ ($di/dt = 11.3 \text{ A}/\mu\text{s}$)

In addition, the specific arc resistance values of the laminar and turbulent flow section are compared in figure 9. The results from both the reference case and the investigations in this research work indicate that in the vicinity of current zero the values of the specific resistance as well as its temporal growth rate after current zero are significantly higher in the turbulent arc section (especially section *b*, position *c* in the reference case respectively) than in the laminar arc section (section *a*, position *a* and *b* in the reference case) [2].

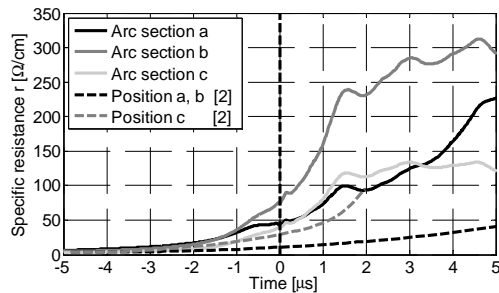


Fig. 9 Specific arc section resistance values r for successful current interruption from [2] and from test series with $L = 0.22$ mH ($di/dt = 11.3$ A/ μ s)

Differences in the observed values of the relative and absolute specific resistance result from the significantly higher quenching gas pressure and the higher current steepness values di/dt applied in the reference case. Furthermore, the length of the laminar flow section upstream of the nozzle throat is $l = 20$ mm in the reference case and thus different from the length of the laminar arc section investigated in this research work. This difference is caused by the given minimal distance between two sensor layers and the geometry of the used nozzle.

Furthermore the analysis of the resistance distribution in the reference case is performed in discrete cross-sections, i.e. resistance values in discrete positions, whereas with the capacitively coupled measuring principle potential values for discrete measuring positions are determined leading to resistance values distributed into different spatially extended arc sections. This characteristic of the capacitive measuring principle leads to an averaged measurement of different physical effects which occur in spatially non-extended sections (e.g. the transition of laminar flow into turbulent flow downstream of the nozzle throat) and is dependent on the distance between two sensor layers, i.e. the spatial resolution of the measurement system.

6. CONCLUSION AND OUTLOOK

A measurement system for the determination of the spatial arc resistance distribution of an axially blown switching arc has been analyzed concerning the quality of the results. It is observed that during the high current phase the arc resistance in the laminar flow section accounts for the dominating percentage of the total arc resistance. First in the vicinity of current zero the relative laminar arc resistance decreases and the relative resistance in the turbulent flow section significantly increases. Thus the dominant role of the turbulent arc section relevant to the decision of successful or non-successful current interruption is confirmed. Comparing the measurements to the results from a reference case a general agreement is observed. In future investigations the measuring accuracy of the measurement system could be increased by detailed analysis of arc instabilities. Here further information on the arcing behaviour could be obtained from optical investigations, for example by means of viewing slots.

ACKNOWLEDGEMENT

The authors are thankful to ABB Corporate Research Center Switzerland for the topical discussions and the financial support of this research work.

REFERENCES

- [1] M. Hoffacker, "Method for the spatially resolved measurement of the resistance distribution of an axially blown switching arc", Ph.D. Thesis (in German), RWTH Aachen University, 2012.
- [2] W. Hermann, U. Kogelschatz, L. Niemeyer, K. Ragaller, E. Schade, "Investigation on the Physical Phenomena around Current Zero in HV Gas Blast Breakers", IEEE Transactions on Power Apparatus and Systems, Vol. PAS-95, No. 4, July/August 1976.
- [3] M. Hoffacker, T. Frehn, "Measurement of the Spatial Arc Resistance Distribution of an Axial Blown Switching Arc", XIXth International Conference on Gas Discharges and Their Applications, Beijing (China), 2012.